Combined Numerical/Experimental Approach for Rivet Strength Assessment

F. Previtali *, M. Anghileri, L.-M. L. Castelletti and A. Milanese

Politecnico di Milano, Dipartimento di Ingegneria Aerospaziale, Milan, Italy

* mail to: infolast1@aero.polimi.it

Summary:
The failure mechanism of common aeronautical structures is influenced by the crash behaviour of the riveted joints. Therefore, crashworthiness analyses of aeronautical structures require accurate models of the joints under crash conditions for a correct prediction of the crash behaviour of the structure.

In this work, a method to create reliable FE models able to reproduce the behaviour of rivets under crash conditions is introduced.

Using explicit FE codes, it is common practice to model rivets and bolts with rigid links or beams, and adopt as a failure criterion the allowable forces envelope obtained for a single rivet after tests [1]. It is shown here that numerical simulations of tests carried out on a single rivet under different loading conditions can be used to characterise the crash behaviour of riveted joints in place of expensive and time-consuming test campaigns.

A specific test device was built in order to apply multi-axial loads to a single rivet and perform tests to evaluate the behaviour of a rivet under different loading conditions: from pure shear to pure tension.

Numerical simulations of the single rivet test were then carried out using LS-Dyna [1] to reproduce experimental test and to validate the numerical model of the rivet.

The rivet was discretised with solid eight-node elements and the piecewise linear plasticity material model was initially used. However, different constitutive laws were then used to characterise areas with either compressive or tensile loads. The whole loading process, from bucking to failure was simulated. Numerical results and test data were compared and it was observed that the numerical models are able to correctly represent the behaviour of a rivet after a tuning of the material parameters and therefore can be used to characterise a riveted joint.

At this stage of the research, only quasi-static loading conditions were considered. This assumption allowed reducing the number of parameters that affects the calculations thus simplifying the model set-up. Future works will investigate the effect of strain rate to reproduce crash conditions.

Keywords:
Aircraft Joints, Rivet Modelling, Multi-axial tests, Numerical model

1 INTRODUCTION

Crashworthiness analyses of aeronautical structures require accurate models of the riveted joints. Since the crash failure mechanism of the aeronautical structures is affected by the behaviour of joints, for a correct prediction of the crash behaviour of these structures it is important to model with a degree of accuracy riveted joints under crash conditions.

In this work, a method is introduced to create reliable FE models able to reproduce the behaviour of rivets under crash conditions.

Using nonlinear explicit FE codes, rivets are usually modelled with rigid links or beams and using as failure criterion the allowable forces envelope obtained for a single rivet after tests [1]. In this research, it is shown that detailed finite element simulations can be used as a tool to characterise the crash behaviour of riveted joints in place of expensive and time-consuming test campaigns.

2 EXPERIMENTAL TESTS

Experimental tests were performed to investigate the behaviour of a type of rivet widely used in aircraft industry and to collect reliable data to validate numerical models of riveted joints. To this extent the device shown in Figure 1 was used.

The rivets were installed on a steel support using a pneumatic riveter. The supports consist of two square blocks shaped to house the rivet that were fixed to the two disk quarters by means of a total of eight screws.

The supports are stiffer than the rivets and designed to avoid plastic deformations during bucking process and test. However, since it is impossible to avoid completely micro-cracks and plastic deformations (bare-eye invisible), the supports were substituted after five tests.

The two disk quarters were constrained to the test rig in various angles using a pin. In this way the global force was resolved in two components in the support referential (tensile force f_N and shear force f_S) as a function of the angular inclination. Five inclinations of the applied load are feasible: 0° (pure tension), 30°, 45°, 60° and 90° (pure shear).

The tests were performed using the MTS 858 Mini Bionix II quasi-static tension/compression machine (left hand side of Figure 1) which allowed acquiring directly the force/displacement curve. On the right hand side of Figure 1 is shown a detail of a test with an inclination angle of 45°.

Figure 1: The devices used for the tests on the rivets (inclination angle 45°)

For each inclinations of the applied load, several tests were undertaken to obtain better statistical values.

In Figure 2 the load/displacement curves collected for the axial and shear tests are shown while the rivets after the test with different loading conditions are shown in Figure 3. In particular, it was observed that for all loading conditions the failure occurred at the shaft while no failure appeared in the head or in the shop-head.
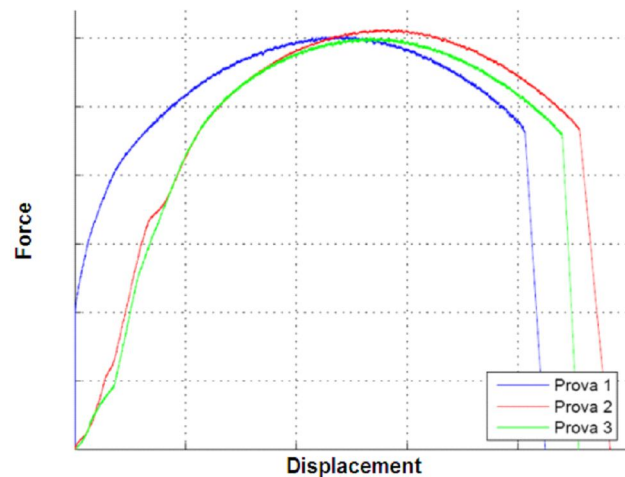
Experimental data were plotted in the S_N/S_S plane (Figure 4) – where S_N is the tensile force and S_S is the shear force at failure and then interpolated with the equation that is used to characterise the failure of either a single rivet or a riveted joint [1]:

$$\left(\frac{|f_N|}{S_N}\right)^n + \left(\frac{|f_S|}{S_S}\right)^m = 1 \tag{1.}$$
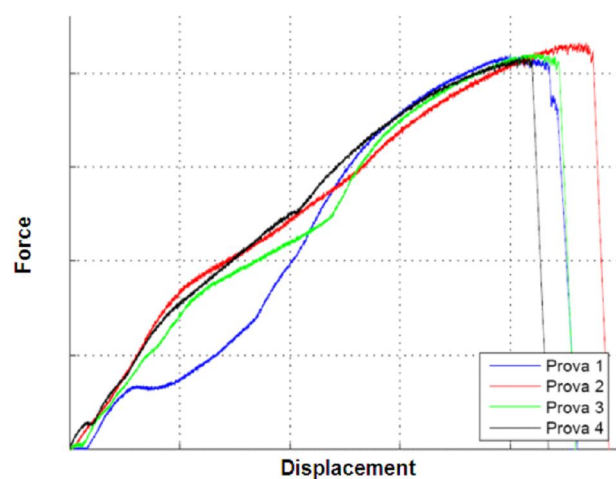
where m and n are parameters to be determined depending on the interpolated data.

When a simpler, yet less accurate, equation is desired or when data of tests with different loading angles are not available, parameters m and n are usually set equal to 2 thus obtaining the equation of an ellipse.

Experimental data and their interpolating curves are shown in Figure 4. It is possible to note that the super-ellipse interpolation gives a more precise representation of the test data. However, the ellipse interpolation might represent an acceptable alternative.

(A) Axial test

(B) Shear test

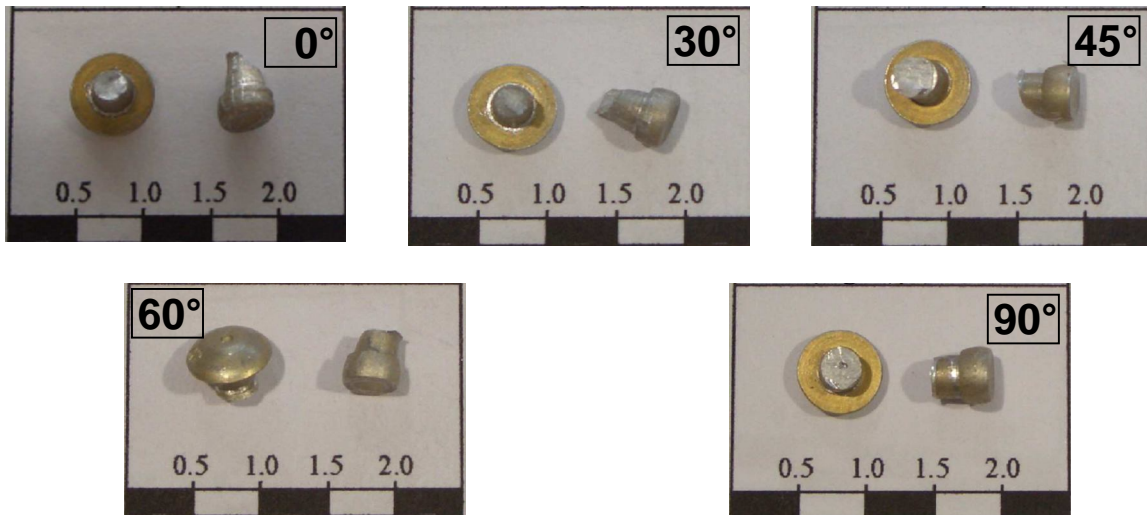*Figure 2: force versus displacement plot for (A) axial and (B) shear tests.*

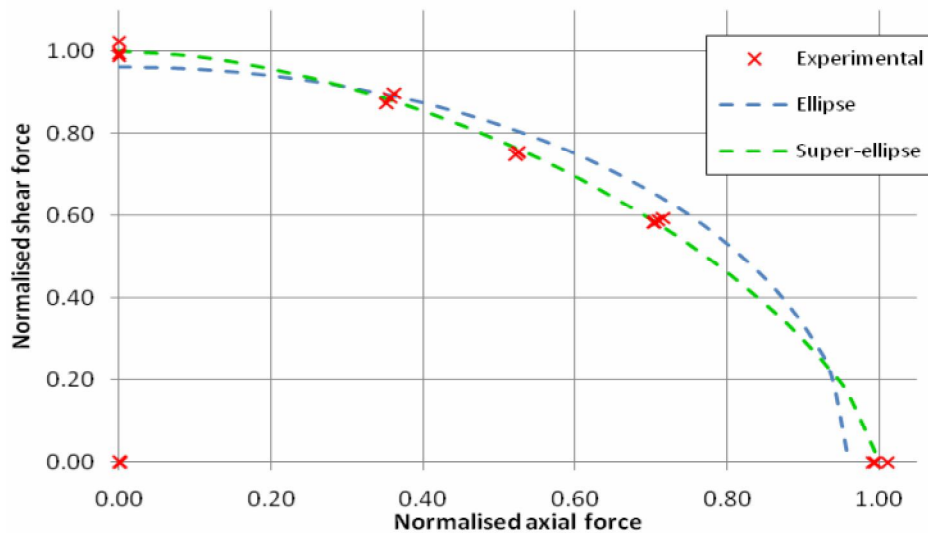Figure 3: pictures of rivets after the test for different loading conditions.

Figure 4: experimental data and interpolating curves.

	S_N	S_T	m	n
Ellipse	2.9	2.0	2.0	2.0
Super-ellipse	3.0	2.1	1.7	1.5

Table 1: parameters of the interpolation.

3 NUMERICAL SIMULATIONS

In order to numerically reproduce experimental tests, simulations have been performed with LS-Dyna 971 [1].

3.1 Model description

The rivet was modelled with fully integrated quadratic eight-node solid elements with nodal rotations (ELFORM 3).

A material model with piecewise plastic field definition (*MAT24) was used. This model allowed defining failure criteria based on maximum equivalent strain.

Due to the solid element formulation adopted, it was not possible to define additional failure criteria (*MAT_ADD_EROSION). As a result, it was not possible defining different failure criteria or values for compressive and tensile stresses.

In order to model the different behaviour of the material in compression and tension and to avoid element failure during the bucking phase, various constitutive laws were investigated.

In particular, the results obtained by defining various curves for the plastic field of the material model adopted (*MAT_24) are shown in Figure 5.
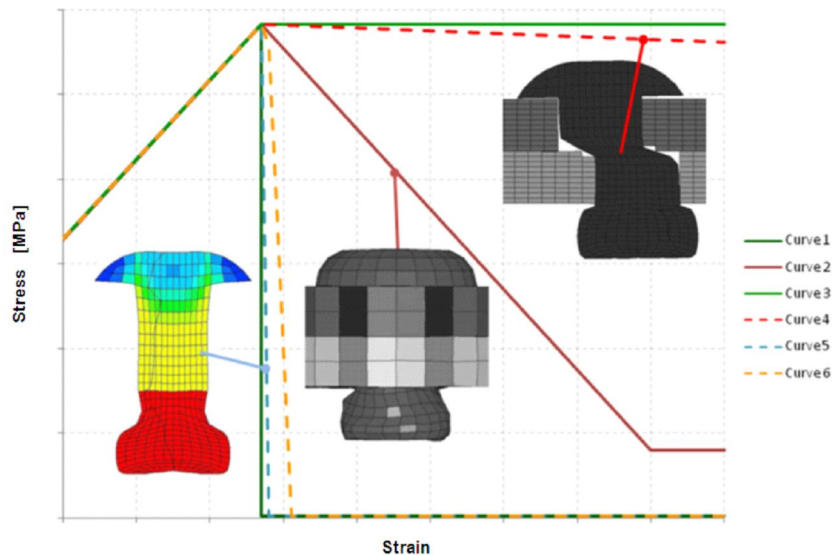

Figure 5: material constitutive laws.

The *curve #1* correctly describes the material behaviour in tension. However, due to the high deformation occurring during the bucking phase, the shop head has a very low residual strength and therefore the rivet is not able to carry loads.

The *curve #2* represents a reasonable trade-off between compressive (no failure) and tensile behaviour. However, because of the negative slope of the curve after the failure strain, the elements deform in an unrealistic way and the shop head deformation is not symmetrical.

The *curve #3* is characterised by a constant value of the stress after reaching the ultimate stress. At the end of the bucking phase, because of the null slope of the curve after the ultimate stress, the elements start returning to the initial, undeformed configuration.

The *curve #4*, characterised by a very small negative slope, allows good results during the bucking phase. In addition, during axial loading test, the rivet necking limits the maximum force to the correct value. However, when simulating the shear loading, the elements deformed excessively and started working in under axial load leading then to incorrect results.

In view of these results, the body of the rivet was eventually divided into two parts (Figure 6): for the head and the shop head, the stress/strain curve #4 was used; for the central part, the stress/strain curve #5, which is characterised by a low residual stress after reaching the reference failure strain, was used. However, because of the sharp change of the slope after the failure strain, the shaft of the rivet experienced some locking phenomenon which prevented it from further deforming and thus failing. In order to avoid these numerical instabilities, a smoother slope change was then adopted (curve #6).

The fillet between the head and the shaft was not modelled to limit the calculation time. Thus, the stress/strain curve #5 was used also to the top part of the shaft (Figure 6) to avoid failure to be initiated by unrealistic stress concentrations in this area.

Other material models were tested, including the Gurson's constitutive law. However, the piecewise plastic model described above provided the best results. Moreover, because of the small number of parameters required, this material model was deemed the most suitable for applications where few data on the materials are available.

As a future work, to improve the results obtained here, a user-defined material model with different compression-tension behaviour and a failure criterion based on stress tri-axiality will be implemented.
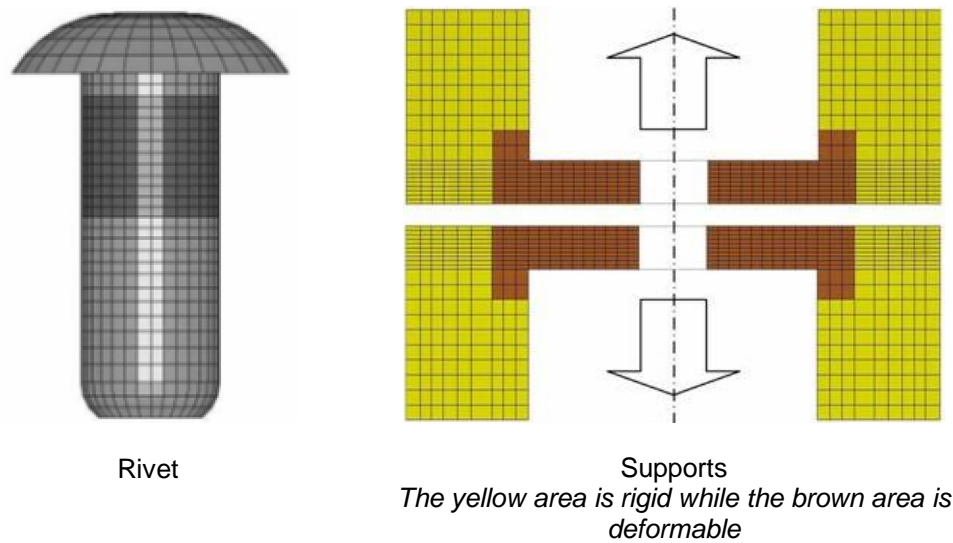
Rivet

Supports
The yellow area is rigid while the brown area is deformable

Figure 6: FE model of rivet and steel supports.

The supports were modelled with eight node solid elements. Since the external part is stiffer than the rest of the structure, it was modelled as a rigid body. On the contrary, an elastic material model with piecewise plastic field (*MAT24) was used for the central part of the support. Also a part of the stiffer zone was modelled as deformable to prevent non-physical behaviour in the deformable-rigid interface (see Figure 6).

The disk quarters and other components of the test device were not modelled to reduce the calculation time.

Nodes were created in correspondence of the hinges and connected to the supports with rigid elements. Single point constraints (not shown in Figure 6) were then applied so that the loads were introduced like in the actual tests: one support fixed and the other one moved with a prescribed displacement (*BOUNDARY_PRESCRIBED_RIGID).

Loads and constraints were applied to the structure by means of zero-length springs (characterised by a constant stiffness) to model the uncertain due to the finite stiffness of the test device.

The bucking tool was rigid and modelled with eight-node solid elements.

Automatic surface to surface contacts (*CONTACT_AUTOMATIC_SURFACE_TO_SURFACE) were used for both the contacts between the rivet and the supports and the contact between the rivet and the bucking tools.

Initially, to avoid zero energy modes, an hourglass control was defined (*CONTROL_HOURGLASS). As a result the hourglass energy was high and, therefore, for the solid elements of the rivet, the fully integrated formulation (ELFORM 3) was adopted. For the deformable part of the support, a selective fully integrated formulation (ELFORM 2) was adopted because hourglass was less critical.

Simulations consisted of two parts: the bucking process and the actual test.

The bucking process does not depend on the test to be simulated and therefore the simulation of this phase was run only once and the results used as a starting point for all the test simulations.

In particular, since LS-Dyna allows restarting the simulation and modifying some cards from the original input file, the prescribed motion curve was changed and different test scenarios were simulated without the need to re-run the bucking phase.

However, it was not possible to adopt the same approach to change the stress-strain curve of a material because modifications of the curve used to define the material constitutive law were not allowed.

The duration of an actual static test is too long for the typical time-step of an explicit calculation. Therefore, in an effort to limit the CPU time required by the simulation, the termination time was reduced by increasing the velocity of the displacements. Since no strain rate dependency was defined and the kinetic energy was negligible, this approximation did not affect the accuracy of the results.

In addition, the mass-scaling option was used to increase the time-step (*CONTROL_TIMESTEP). Since inertial effects were negligible, no significant errors were observed even when relevant masses were added and the overall calculation time was reduced by several orders.

Initially, the symmetry of the problem was exploited and only half model of the test was created to reduce the calculation time. However, various differences were observed when comparing the results obtained with the complete and the simplified model. It was thus decided to use the complete 3D model.

The value of the loads applied to the rivet was measured from both the interface forces file (*DATABASE_RCFORC) and the boundary conditions forces files (*DATABASE_BNDOUT).
The results were processed with a 2nd order Butterworth filter (cut-off frequency 1000 Hz) to reduce spurious oscillations and cut high frequency noise.
Since inertial energy is negligible, the two sets of results showed small discrepancies and this was also considered a point to prove the reliability of the model.

3.2 Results of the simulations

The sequence from the bucking to the failure of the rivet is shown in Figure 7 referring to the test with inclination angle of 45°.
The failure mechanisms obtained in the simulations reproducing the tests with different load angles are shown in
Figure 8. In particular, a section cut of the rivet under different loading conditions before failure is shown. The fringes show the plastic strain in the elements thus helping visualizing the failure mode.
The high deformation values in the shop-head are due to the bucking process.
The stress concentrations in the shaft-head connection are caused by the suppression of the fillet in the FEM model. However, because of the material model adopted for in this area, the stress concentration does not initiate the failure.

As apparent in
Figure 8, numerical simulations correctly reproduce the failure mechanism observed during experimental tests (Figure 3), with the exception of the pure tension load case.
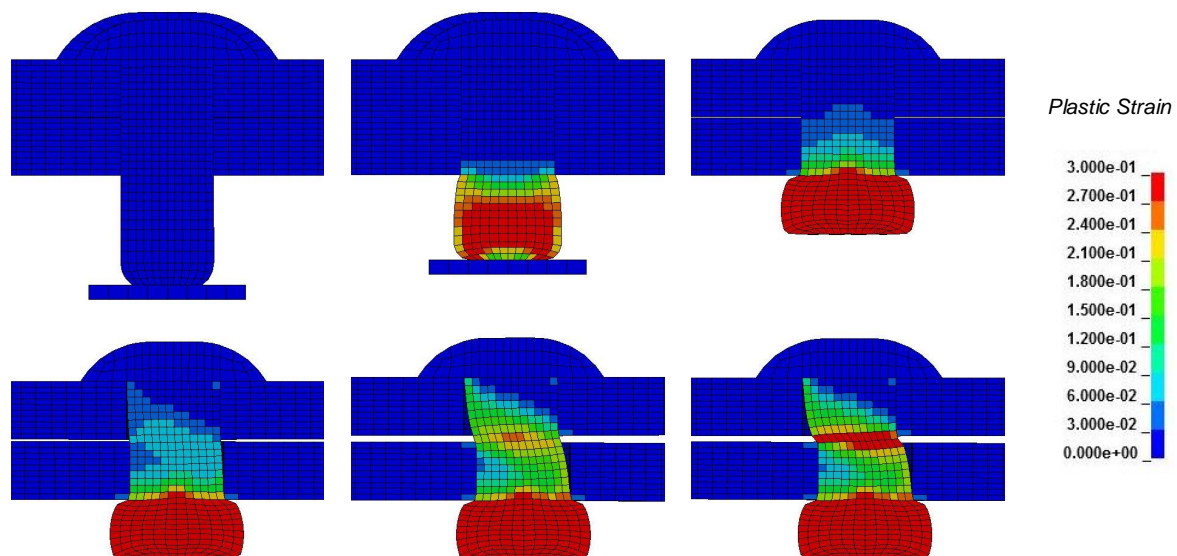

Figure 7: Sequence from the numerical simulations of the test with a 45° load angle.

The maximum forces numerically obtained were then compared with the experimental data. It was observed that numerical results were lower than the experimental ones. This discrepancy is due to the fact that the mechanical properties of the rivet's material were obtained from values found in the datasheets provided with the rivets. The data reported in these datasheets are usually the minimum guaranteed and therefore the results obtained are *conservative*.

Instead of adjusting the material parameters, numerical results were scaled with a constant coefficient to match the test data. After that, simulation results show a good correlation with experimental data (Figure 9).
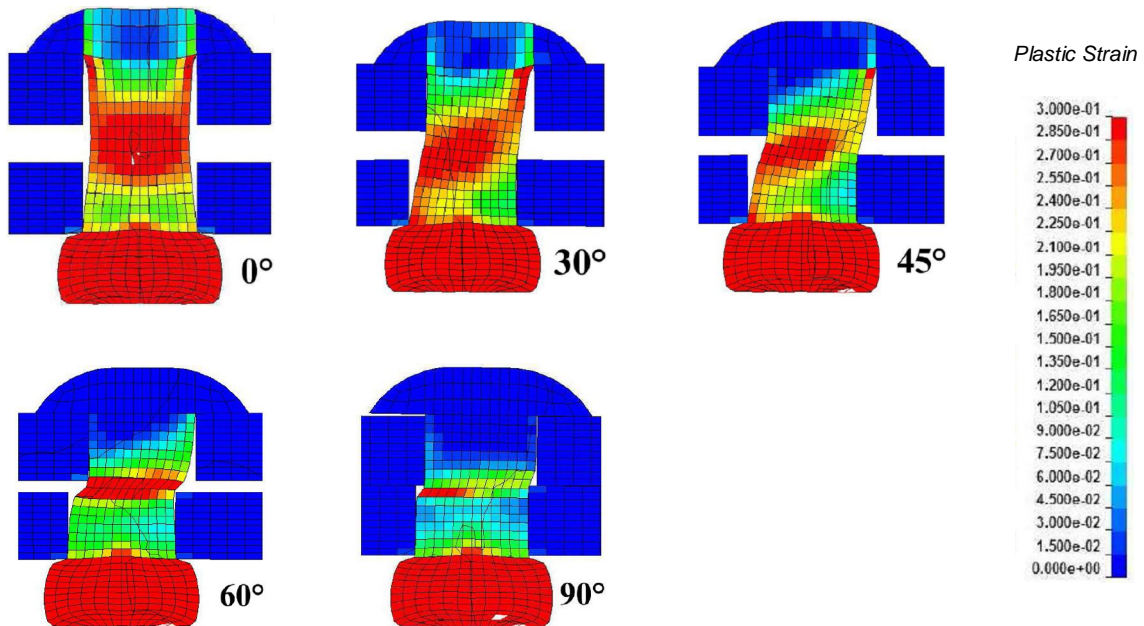

Figure 8: plastic deformation of the rivets just before the failure for different loading conditions.
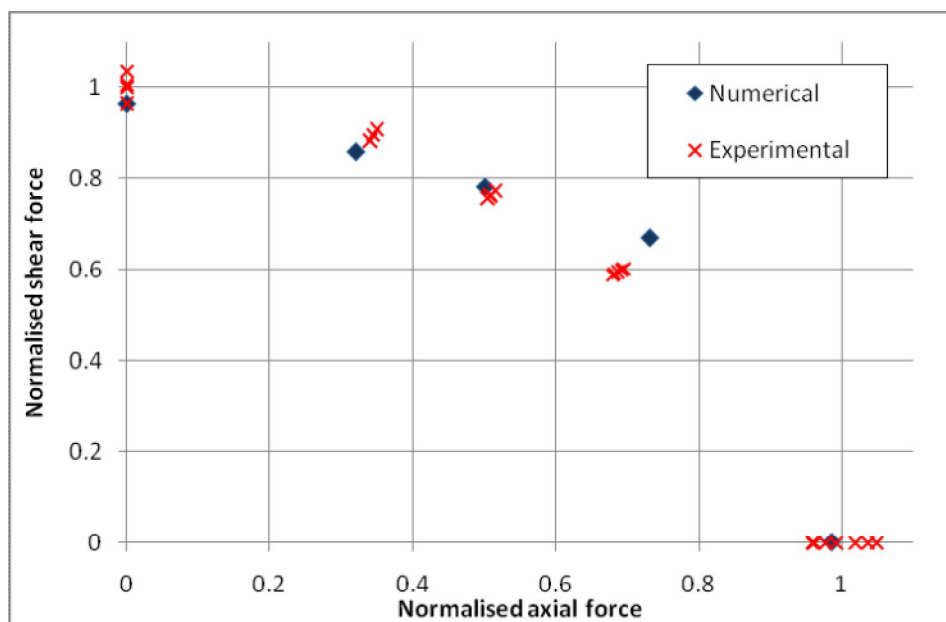

Figure 9: comparison between experimental data and numerical results.

4 CONCLUSIONS

For a correct prediction of the crash behaviour of the aircraft structures it is important to model with a degree of accuracy riveted joints under crash conditions.

The aim of this work was to develop a method for characterising the numerical model of a rivet that allows predicting its behaviour under crash conditions.

Experimental tests and numerical simulations were carried out. In order to characterise the behaviour of the rivet various material models were considered and, eventually, a reliable numerical model validated against experimental tests was obtained.

It is shown that the numerical model can be used in place of expensive, time consuming and difficult to perform tests to obtain the curve that characterise the failure of rivets under multi-axial state of stress in explicit FE codes.

Further works are though necessary to include in the model the influence of the strain rate and the dependability of the data provided with the rivets.

5 LITERATURE

[1]   J. O. Hallquist: "LS-DYNA Theory Manual", Livermore Software Technology Corporation, March 2006.
[2]   B. Langrand, L. Patronelli, E. Deletombe, E. Markiewicz, P. Drazétic: "An alternative numerical approach for full scale characterization for riveted joint design", Aerospace Science and Technology, 2002.
[3]   B. Langrand, E. Deletombe, E. Markiewicz, P. Drazétic: "Riveted joint modeling for numerical analysis of airframe crashworthiness", Aerospace Science and Technology, 2001